Estimation of Reservoir Capacity Using Remote Sensing Data – A Sub-pixel Classification Approach

JEYAKANTHAN, V.S.

Scientist-D, Deltaic Regional Centre, National Institute of Hydrology,
Siddartha Nagar, Kakinada-533 003, Andhra Pradesh.
jeyakanthan05@gmail.com

Abstract: *Sediments carried by the rivers are deposited in the reservoirs and cause several detrimental effects, which include loss of storage capacity, upstream aggradations, effect on water quality and damage or impairment of hydro-equipments. The deposition of sedimentation not only reduces the capacity but also the water-spread of the reservoir. Satellite data has long been in use to estimate the water-spread area at different elevations of a reservoir, which in turn can be used to quantify the capacity of the reservoir. This methodology to estimate the capacity of a reservoir using remote sensing data involves hard or per-pixel based classification to delineate the water-spread area at a particular elevation. One of the limitations of this approach is that the border pixels, representing soil class with moisture, are classified entirely as water pixels, thereby giving inaccurate estimate of the water-spread area. To estimate the water-spread area of Nagarjuna Sagar reservoir accurately, the sub-pixel or linear mixture model (LMM) approach has been adopted in this study. The sub-pixel approach uses a linear mixture model of the spectra to quantify the proportions of water and other classes present in each of the border pixels of the reservoir. IRS-1C and 1D satellite image data (24m) of eight optimal dates ranging from minimum draw down level (MDDL) to full reservoir level (FRL) were used to estimate the water-spread area of the reservoir. The extracted water-spread areas using per-pixel and sub-pixel approaches were in turn used to quantify the capacity of the Nagarjuna Sagar reservoir. The estimated capacity of the Nagarjuna Sagar reservoir using per-pixel and sub-pixel approaches was 8101.63 Mm^3 and 8014.49 Mm^3 respectively.*

Keywords: *Reservoir, Water-spread area, Capacity estimation, Per-pixel and Sub-pixel approaches*

1. Introduction:

Natural processes, such as erosion in the catchment area, movement of sediment and its deposition in various parts of the reservoir, require careful consideration in the planning of major reservoir projects. The silt that is deposited at different levels reduces the storage capacity of the reservoir [1, 2]. Reduction in the storage capacity beyond a limit prevents the reservoir from fulfilling the purpose for which it is designed. Periodic capacity surveys of the reservoir help to assess the rate of sedimentation and reduction in storage capacity. Conventional techniques for the estimation of the capacity of a reservoir, such as hydrographic survey and inflow-outflow approaches, are cumbersome, time consuming and expensive, and they involve significant manpower. As an alternative to conventional methods, the remote sensing technique provides cost- and time-effective estimation of the live capacity of a reservoir [3, 4]. Multi-date satellite remote sensing data provide information on elevation contours, in the form of water spread area, at different water levels of a reservoir. The water spread area thus interpreted from the satellite data is used as an input into a simple volume estimation formula to calculate the capacity of a reservoir. Such work has been reported by [5] for the Malaprabha Reservoir in India, [6] for the Poondi Reservoir in India, [7] for the Bargi Reservoir in India and [4] for the Bhakra Reservoir in India.

For quantification of the capacity of a reservoir, the only thematic information that has to be extracted from the satellite data is the water-spread area at different water levels of the reservoir [8, 9]. The different approaches such as maximum likelihood, minimum distance to mean classification and band threshold method, to delineate various thematic information from the remote sensing digital data adopt the per-pixel based methodology and assign a pixel to a single land cover type [10, 11] whereas in reality, a single pixel may contain more than one land cover (known as a mixed pixel). Mixed pixels are common especially near the boundaries of two or more discrete classes [12, 13]. The boundary pixels of the water-spread area that are mixed in nature, representing soil, vegetation class with moisture are also classified as water pixels when a per-pixel based approach is applied, thereby producing inaccurate estimate of the water-spread area. To accurately compute the water-spread area to the maximum possible extent, thereby reducing the error in the estimation of capacity of a reservoir, a sub-pixel or linear mixture model (LMM) approach has been chosen for classifying the boundary pixels of water-spread area from different water levels of Nagarjuna Sagar reservoir located in Andhra Pradesh state of India.

2. Study reservoir:

Nagarjuna Sagar is one of the world's largest masonry dam built across the river Krishna in Nagarjuna Sagar town, Nalgonda District of Andhra Pradesh, India, between 1955 and 1967. The capacity of Nagarjuna Sagar reservoir at FRL (Full Reservoir Level) during impoundment was 11,472 million cubic metres. The dam is 490 ft (150 m) tall and 1.6 km long with 26 gates which are 42 ft (13 m) wide and 45 ft (14 m) tall. The geographic region pertains to the reservoir experiences hot and dry summer throughout the year except during the South-west monsoon season. The monsoon season is from June to September and retreating monsoon or the post monsoon season is during October to November. The average rainfall in the district is 772 mm. 71% of the annual rainfall is received during south-west monsoon. The mean daily maximum temperature is about 40^{o} C and the mean daily minimum is about 28^{o} C. The soils in and around the study reservoir mainly comprise loamy sands, sandy loams and sandy clay loams. In the areas of flat topography and alongside the river Krishna and its tributaries comprises mainly of black cotton soil.

2.1 Satellite Data Used:

The image data used in this study were obtained by the Indian Remote Sensing (IRS) satellites IRS-1C & 1D (LISS-III sensor) which provides a spatial resolution of 24 m and spectral resolution in four different bands (0.52-0.59, 0.62-0.68, 0.77-0.86, 1.55-1.70 μm). The different dates of satellite data used and the respective water level during the pass of the satellite over the reservoir are given in Table 1. Reservoir water level data and the hydrographic survey details have been collected from the Nagarjuna sagar reservoir authority responsible for the maintenance and operation of the reservoir.

Table. 1 *Details of satellite data used and the water level during the pass of the satellite over the reservoir*

Sl.No.	Name of the Satellite	Date of Satellite Pass	Reservoir Elevation (m)
1.	IRS-1C	23.10.2001	175.32
2.	IRS-1D	12.12.2001	166.68
3.	IRS-1D	24.12.2001	164.74
4.	IRS-1D	25.02.2002	157.03
5.	IRS-1D	14.09.2002	156.94
6.	IRS-1D	11.05.2002	154.72
7.	IRS-1D	27.11.2002	153.19
8.	IRS-1D	22.12.2002	152.28

3. Methodology:

The changes in water-spread could be accurately estimated by analyzing the areal spread of the reservoir at different elevations over a period of time using the satellite image data [9,1]. Both the per-pixel and sub-pixel or Linear Mixture Model (LMM) approaches have been used in this study to extract the water-spread area of the reservoir. Estimated water-spread areas were used in a simple volume estimation formula to compute the storage capacity of the reservoir. Estimation of water-spread area and computation of capacity of the reservoir using per-pixel and sub-pixel approaches are discussed in the following sections.

3.1 Geo-referencing of satellite data:

In the IRS-1C and 1D (LISS-III) satellite data the reservoir water-spread area was free from clouds and noise in all of the eight images used. The image scene of 23rd October 2001 was geo-referenced with respect to 1:50,000 survey of India topographic maps. The geo-referencing was done using ployconic projection and nearest neighborhood re-sampling technique to create a geo-referenced image of pixel size 24m x 24m. Subsequently the other satellite images corresponding to various water levels were also registered with the geo-referenced image using the image to image registration technique. In every image 20 to 25 ground control points were used, which resulted in a root mean squared error (RMSE) of 0.15 to 0.18 of a pixel.

3.2 Per-pixel based approach:

The most widely used method for extracting information on the surface cover from remotely sensed data is image classification. Digital image classification uses the spectral information represented by the digital numbers in one or more spectral bands and attempts to classify each individual pixel (per-pixel approach) based on this spectral information. A number of commonly used per-pixel based classifiers exist including the maximum likelihood, the minimum distance to mean, mahalanobis distance and the parallelipiped classifiers. A detailed account of these and the other classifiers can be found in [14, 15]. The objective of the per-pixel based classifiers is to assign all pixels in the image to particular classes or themes (e.g. water, forest, urban, agriculture). The resulting classified image is comprised of a mosaic of pixels, each of which belongs to a particular theme and is essentially a thematic map of the original image. The per-pixel based classification can be divided into unsupervised and supervised classification. The underlying requirement of supervised classification techniques is that the user/analyst has sufficient pixels (training sets) available for which the true class is known. From these pixels, representative signatures can be developed for those classes for subsequent classification.

The steps involved in supervised classification include (i) identification and decisions relating to the set of classes/cover types into which the image is to be segmented, (ii) choice of the representative pixels for each of the desired set of classes (*i.e.*, construct the training data), (iii) estimation of the parameters (*eg*. class signatures) of the classification algorithm from the training data, (iv) use of the classifier to label (or 'classify') every pixel in the image into one of the desired/predetermined cover types, (v) production of thematic maps which contain the results of the classification, and (vi) determination of the accuracy of the classification by comparing the output to ground truth data. In this study, water-spread area was extracted using the most commonly adopted maximum likelihood classification approach. The estimated water-spread was in-turn used in a volume estimation formula to compute the capacity of the reservoir.

3.3 Sub-pixel based approach:

The basic assumption of linear mixture model is that the measured reflectance of a pixel is the linear sum of the reflectance of the components that make up the pixel. The basic hypothesis is also that the image spectra are the result of mixtures of surface materials, shade and clouds, and that each of these components is linearly independent of the other [16, 17]. Linear unmixing also assumes that all the materials within the image have sufficient spectral contrast to allow their separation. In soft classification, the estimated variables (the fractions or proportions of each land cover class) are continuous, ranging from 0 to 100 percent coverage within a pixel. [18] and [12], proposed a mathematical expression for linear spectral unmixing. The theory behind this is the contribution of a series of end-members present within a pixel to its spectral signature. Hence, the spectral signature of a pixel would be derived from the sum of the products of the single spectrum of the end-members it contains, each weighted by a fraction plus a residue which would be explained by the following mathematical model:

$$R_i = \sum f_k R_{ik} + E_i \qquad (1)$$

where $\sum f_k = 1$ (2)

and $0 \leq f_k \leq 1$ (3)

i = 1, . . ., m (number of spectral bands)
k = 1,. . ., n (number of endmembers)
R_i = Spectral reflectance of band i of a pixel which contains one or more endmembers
f_k = Proportion of endmember k within the pixel
R_{ik} = Known spectral reflectance of endmember k within the pixel on band i
E_i = Error for band i (Difference between the observed pixel reflectance R_i and the reflectance of that pixel computed from the model).

Equations 1 and 2 introduce the constraints that the sum of the fractions are equal to one and they are non-negative. To solve f_k, the following conditions must be satisfied: (i) selected endmembers should be independent of each other, (ii) the number of endmembers should be less than or equal to the spectral bands used, and (iii) selected spectral bands should not be highly correlated.

In this study, the linear spectral unmixing is adopted based on the equations described below to segregate the actual information within a pixel of an image

$$\begin{aligned} R1 &= F_{water} * R1_{water} + F_{Veg} * R1_{Veg} + F_{Soil} * R1_{Soil} + \varepsilon 1 \\ R2 &= F_{water} * R2_{water} + F_{Veg} * R2_{Veg} + F_{Soil} * R2_{Soil} + \varepsilon 2 \quad (4) \\ R3 &= F_{water} * R3_{water} + F_{Veg} * R3_{Veg} + F_{Soil} * R3_{Soil} + \varepsilon 3 \end{aligned}$$

Where,
→R1, R2 and R3 represent the signal recorded at the satellite in the green, red and NIR bands of the LISS-III sensor.
→F_{water}, F_{Veg} and F_{Soil} are the fraction of the pixel covered by water, vegetation, and soil.
→$R1_{water}$, $R2_{water}$ and $R3_{water}$ represent the reflectance of water in each of the three spectral bands.
→$R1_{Veg}$, $R2_{Veg}$ and $R3_{Veg}$ represent the reflectance of vegetation in each of the three spectral bands.
→$R1_{Soil}$, $R2_{Soil}$ and $R3_{Soil}$ represent the reflectance of soil in each of the three spectral bands.
→ε1, ε2 and ε3 are the error components of band 1, 2, and 3.

The system of linear equations shown above can be solved by a least square solution which minimizes the sum of squares of errors.

The sub-pixel based approach was applied to find out the proportion or fraction of water class that exits in the periphery pixels of the reservoir. The first step executed in the sub-pixel approach was, selection of end-members. In general the border pixels may contain any combination and proportions of water, vegetation and soil classes, therefore these three classes were chosen to collect the end-members. Scatter plot method was used to identify the end-members. The identified end-member spectra were supplied as input to the linear mixture model (LMM) approach. The output of the model run contains three images known as water, soil and vegetation fraction images. Description of the fraction images is given in section 4.2.

3.4 Computation of volume between successive water levels:

Traditionally the reservoir volume between two consecutive reservoir water levels, was computed using the prismoidal formula, the Simpson formula and the trapezoidal formulae [19]. Of these, the trapezoidal formula has been most widely used for computation of volume [20, 21]. The water-spread area estimated using sub-pixel approach was used as an input in the volume estimation formula to find out the, volume at different water levels of the reservoir. In this study the volume between two consecutive reservoir water levels was computed using the following trapezoidal formula.

Trapezoidal Formula: $V = H/3\ (A1 + A2 + \sqrt{A1*A2})$ (5)

Where V is the volume between two consecutive water levels. A1 and A2 are the water-spread area at the reservoir water level 1 and 2 respectively and H is the difference between these two water levels.

3.5 Computation of storage capacity of the reservoir:

The volume computed between different water levels (i.e from Minimum Draw Down Level to Full Reservoir Level) was added up to calculate the cumulative or storage capacity of the reservoir.

4. Results and discussion:

4.1 Computation of reservoir capacity by per-pixel approach:

The supervised classification was performed by using training sets generated for the different landcover classes in and around the reservoirs. Since this exercise involves the estimation of pixels that are occupied by water, it is essential that the training set generation

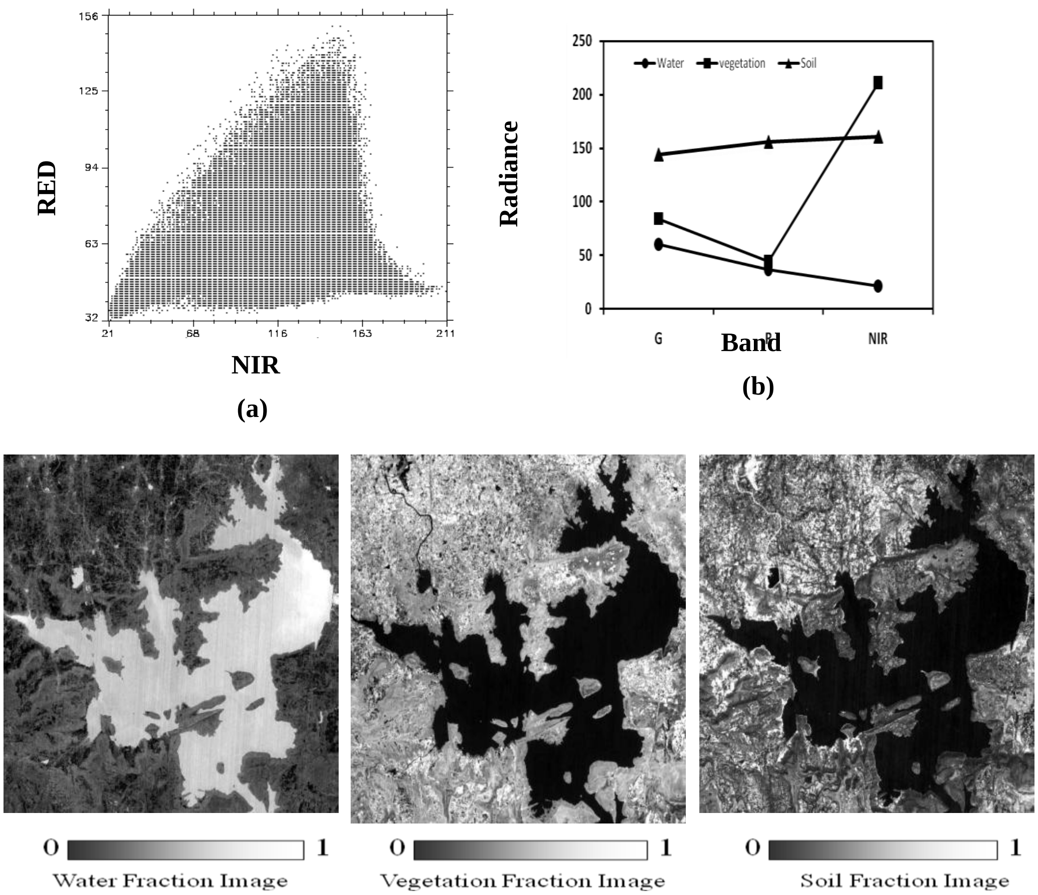

(C)

Figure 1 (a) Feature space plot (NIR *vs* RED), (b) End-member spectra of Soil, Water and Vegetation (c) Fraction images obtained by spectral un-mixing of image data of Nagarjunasagar Reservoir pertaining to the water level 175.32 m (Due to the recurring nature of the fraction images, only figures pertaining to the highest water level is presented).

Table 2: *Capacity estimation of Nagarjunasagar reservoir using the per-pixel and sub-pixel classification approaches (2002)*

Sl. No	Date of Satellite Pass	Reservoir Elevation above m.s.l (m)	Waterspread area - Perpixel approach (Mm^2)	Waterspread area - Subpixel approach (Mm^2)	Cumulative Volume - Perpixel approach (Mm^3)	Cumulative Volume - Subpixel approach (Mm^3)
1.	23.10.2001	175.32	238.55	235.15	8101.63	8014.49
2.	12.12.2001	166.68	203.73	197.03	6192.96	6149.90
3.	24.12.2001	164.74	192.89	194.08	5808.28	5770.53
4.	25.02.2002	157.03	173.75	170.43	4395.53	4366.33
5.	14.09.2002	156.94	166.93	167.42	4380.20	4351.13
6.	11.05.2002	154.72	163.47	155.06	4013.46	3993.26
7.	27.11.2002	153.19	156.69	149.02	3768.56	3760.66
8.	22.12.2002	152.28	153.79	144.11	3627.29	3627.29

should involve careful selection of water pixels. It may noted that the image subset of the study area contains vegetation and soil as the primary land cover classes in addition to the water class. Therefore only three feature/landcover classes were considered to generate training sets for the maximum likelihood classification. Training sets were selected from the center of the reservoir, periphery of the reservoir, from the agricultural fields, shrubs in the peripheral areas and from barren lands representing the soil class. The choice of representative pixels (both number and type) was in accordance with the suggestion of [14]. This procedure was followed carefully for all the eight images pertaining to the Nagarjuna Sagar reservoir. It may be noted that three simple and spectrally distinct classes namely water, soil and vegetation form the basic input for the classification process. The extracted water spread areas and the estimated capacity (8101.63 Mm^3) using per-pixel approach is given in Table 2.

4.2 Computation of reservoir capacity by sub-pixel approach:

The fraction images (Figure 1) generated using the sub-pixel approach described in the methodology section contain a wealth of information about the reservoir. Each fraction image corresponds to a single land cover only. For example, the pixels in the *water fraction image* provide information only on the proportion or amount of water it contains. Likewise the vegetation and soil fraction image provide information on the proportions of the respective classes only. However, in this study the interest is only to know about, the amount of water present in the border pixels of the reservoir.

The value of the pixels in the fraction image ranges from 0 to 1. A pixel from the water fraction image having a value of 0 indicates that there is no water at all in that pixel, whereas a pixel having a value of 0.25 indicates that 25% of the area of the pixel is occupied by water while a pixel value of 1 indicates that 100% of the area of the pixel is occupied by water (i.e the pixel is fully occupied by water). Therefore, for a pixel having a value of 0.72, the area of water occupied by that pixel is 414.72 m^2 (0.72 x 24m x 24m).

The pixels representing the reservoir border which have a minimum value of up to 0.1 in the water fraction image (i.e a pixel contains a minimum 10% of area of water) were isolated from the water fraction image and the area covered by water in these border pixels were estimated. The number of pixels that contains 100% of water was also found out. By summing up the area occupied by these two types of pixels, the total water-spread area, corresponding to a particular water level of the reservoir was computed. This exercise was carried out for all the eight images used in this study. The water-spread area thus estimated was again used as an input in the trapezoidal formula to compute the storage capacity or cumulative capacity of the Nagarjuna sagar reservoir using the sub-pixel classification approach.

Here it is worth mentioning that, a pixel containing 71% of water may be labelled as containing 100% of water by the per-pixel approach. In such case the water-spread area is over estimated. Conversely if the pixel contains 40% of water, then the entire pixel may not be considered as a water pixel. Hence, the water-spread area is under estimated. Such errors due to over estimation or under estimation do not occur in the sub-pixel approach. Thus, the sub-pixel approach reduces the error imposed by the per-pixel approach. The estimated cumulative capacity of Nagarjuna sagar reservoir at the water level 175.32 m (Near FRL) using the sub-pixel approach was 8014.49 Mm^3. The capacity estimated using per-pixel and sub-pixel approaches are given in Table 2.

5. Conclusions:

High spatial-resolution image data enables accurate mapping of the terrain features. The use of high spatial resolution satellite image data, however, is constrained by factors such as cost and less area covered by the sensor. Hence, in hydrological applications estimating water-spread area may be difficult because a reservoir may not be imaged in a single pass of the satellite and atmospheric condition would be different from path to path [22]. An alternative method to overcome such constrains is the use of the sub-pixel based approach. The simplest methodology for such an approach is linear mixture modeling, which has been demonstrated in this study to estimate the capacity of Nagarjuna sagar reservoir in India.

Though the sub-pixel approach found to be a better alternative to per-pixel approach, there are certain limitations such as the spatial location of the fractions within a pixel is unknown. In addition the sub-pixel classifier produces more accurate results only with hyperspectral images. Hence, the use of hyperspectral image data with higher spatial resolution would have yielded better results.

6. Acknowledgement:

The author thanks the Nagarjuna Sagar reservoir authorities for providing the ground based data. The author also thanks Director, NIH for giving permission to publish the paper.

7. References:

[1] Smith, L.C., and Pavelsky, T.M, "Remote sensing of volumetric storage changes in lakes", *Earth Surface Process and Landforms*, Vol.34, pp.1353 – 1358, 2009.

[2] Sreenivasulu, V and Udayabaskar, P, "An integrated approach for prioritization of reservoir catchment using remote sensing and geographic information system", *Geocarto International*, Vol.25, pp.149-168, 2010.

[3] Sabastin, M., Rao, P.P.N., Jayaraman. V., and Chandrasekhar, M.G, "Reservoir storage loss assessment and sedimentation modeling through remote sensing techniques", *Proceedings of 6th Inter. Symp. River sedimentation on Management of Sediment – Philosophy, Aims and Techniques,* New Delhi, India, 1995..

[4] Jain, S.K., Singh, P., and Seth, S.M, "Assessment of sedimentation in Bhakra Reservoir in the western Himalayan region using remotely sensed data", *Hydrological Sciences Journal*, Vol.47, pp.203-212, 2002.

[5] Manavalan, P., Sathyanath, P., Sathyanarayn, M., and Raje Gowda, G. L, "*Capacity evaluation of the Malaprabha reservoir using digital analysis of satellite data"*. Tech. Report no. RC: BO: WR: 001:90, Regional Remote Sensing Service Centre, Bangalore and Karnataka Engineering Research Station, Krishnarajsagar, India, 1990.

[6] Jeyakanthan V.S, Sreenivasalu V, Rao Y.R.S., Ramasastri K.S, "Reservoir Capacity Estimation Using Satellite Data", *International Symposium on Photogrammetry and Remote Sensing, Hyderabad*, 2002.

[7] Goel, M.K., Jain, S.K., and Agarwal, P.K., "Assessment of sediment deposition rate in Bargi Reservoir using digital image processing", *Hydrological Sciences Journal*, Vol.47(S), pp.S81-S92, 2002..

[8] Morris, G.L., and Fan Jiahua, *Reservoir Sedimentation Handbook*, (New York: McGraw-Hill Book Co), 1998.

[9] Peng Dingzhi, Shenglian Guo., Pan Liu, Ting Liu, "Reservoir storage curve estimation based on remote sensing data", *Journal of Hydrologic Engineering*, Vol.11, pp.165-172, 2006.

[10] Jensen R.J., 1996. Introductory Digital Image Processing : A remote sensing perspective, 2nd edition, (London: Prentice Hall International Ltd.,).

[11] Bastin, L. "Comparison of fuzzy c-means classification, linear mixture modelling and MLC probabilities as tools for unmixing coarse pixels", *International Journal of Remote Sensing*, Vol.18, pp.3629-3648, 1997.

[12] Foody, G. M., and Cox, D. P., "Sub-pixel land cover composition estimation using a linear mixture model and fuzzy membership functions", *International Journal of Remote Sensing*, Vol.l5, pp.619-631, 1994.

[13] Oleson, K. W., Sarlin, S., Garrison, J., Smith, S., Privette, L., and Emery, W., "Unmixing multiple land cover type reflectance's from coarse resolution satellite data", *Remote Sensing of Environment*, Vol.54, pp.981-912, 1994.

[14] Mather, P. M., and Koch, M, "Extension of the technique of Principal Component Analysis for use in end-member selection", pp. 346-353, 1997.

[15] Swain, P. H., and Davis, P. H., (Eds.), *Remote Sensing: The Quantitative Approach*, New York, NY: McGraw-Hill, 1978.

[16] Quarmby, N. A., Townsend, J.G.R., Settle.J.J., White, K. H., Milnes, M., Hindle, T. L., and Silleos, N., “Linear mixture modelling applied to A VHRR data for crop area estimation”, *International Journal of Remote Sensing,* Vol.l3, pp.415-425, 1992.

[17] Borel, C. C., and Gerstl, S. A. W., “Non-linear of spectral unmixing models for vegetative and soil surface”, *Remote Sensing of Environment*, Vol.47,pp. 403-416, 1994.

[18] Settle, J.J., and Drake, N.A., “Linear mixing and the estimation of ground cover proportions”, *International Journal of Remote Sensing*, Vol.14, pp.1159-1177, 1993.

[19] Patra, K.C., *Hydrology and Water Resources Engineering*, (New Delhi: Narosa Publishing House), 2001.

[20] Goel, M. K., and Jain, S. K., “Evaluation of reservoir sedimentation using multi-temporal IRS-1A LISS II data”, *Asian Pacific Remote Sensing & GIS Journal*, Vol.8, pp.39-43, 1996.

[21] Rathore, D.S., Anju Choudhary, and Agarwal, P.K., “Assessment of sedimentation in Harakud Reservoir using digital remote sensing technique”, *Journal of the Indian Society of Remote Sensing*, Vol.34, pp.344-383, 2006.

[22] Hung, M.C., and Wu. Y.H., “Mapping and visualizing the Great Salt Lake landscape dynamics using multi-temporal satellite images-1972-1996”, *International Journal of Remote Sensing*, Vol.26, pp.1815-1834, 2005.